FERMILAB-PUB-18-306-AD
ACCEPTED

First measurement of traverse beam optics for the Fermilab Muon Campus using a magnet scanning technique

Joe Bradley

University of Edinburgh, Edinburgh EH8 9AB, United Kingdom

Brian Drendel and Diktys Stratakis

Fermi National Accelerator Laboratory, Batavia IL 60510 USA

(Dated: June 11, 2018)

Abstract

In the following years the Fermilab Muon Campus will deliver highly polarized muon beams to the storage ring of the Muon g-2 Experiment. The transmission fraction of the storage ring has been shown to depend strongly on the transverse optics of the injected beam. Unfortunately, the current diagnostics in the Muon Campus allow only measurement of the beam configuration space which limits how well propagation can be predicted. This paper demonstrates an experimental technique based on a conventional magnet scan to obtain the Twiss parameters at a point, using only beam profiles such that installation of new equipment is not required. A proof-of-principle experiment is presented which shows that this new method is applicable to the Muon Campus, offering a viable approach to optimization of injection in the Muon g-2 Experiment.

This manuscript has been authored by Fermi Research Alliance, LLC under Contract No. DE-AC02-07CH11359 with the U.S. Department of Energy, Office of Science, Office of High Energy Physics.

I. INTRODUCTION

Over the next few years the Fermilab Muon Campus [1] will deliver highly polarized muon beams to the storage ring of the Muon g-2 Experiment [2] with 21 times the statistics of the equivalent Brookhaven experiment [3]. For Fermilab Muon Campus operations, protons accelerated in the upgraded Linac and Booster are adiabatically re-bunched in the Recycler and led to an Inconel target [4,5]. Pions of the appropriate energy are then directed into a Delivery Ring (DR) [6] around which they travel 4 times. The passage through the DR is very beneficial as it will provide enough time for pions to decay into muons and will increase the gap between the “light” muons and “heavy” protons so that the latter can be properly removed with a kicker. The remaining muon beam then travels through a sequence of beamlines which end with a set of 5 magnets known as the final focus, then through an inflector and into the storage ring of the Muon g-2 Experiment.

The aim of Fermilab’s Muon g-2 experiment is to achieve an unprecedented 140 ppb precision measurement of the anomalous magnetic moment of the muon, to do so it will observe the polarization of muon decays in a precisely designed storage ring [7]. This can be accomplished with the considerable challenge of generating, transporting, and focusing large numbers of muons confined to a narrow region of phase space, without significant particle losses or deterioration of beam quality. Unfortunately, the current diagnostics in the Muon Campus beamlines allow only measurement of beam profiles which limits how well propagation can be predicted. Moreover, several numerical studies [8, 9] have shown that the number of stored muons for the Muon g-2 Experiment is largely dependent on the injection parameters, specifically the Twiss parameters. Thus, it is of great importance to develop techniques for measuring the transverse beam optics with a high level of accuracy. This becomes even more challenging for secondary beams (such as pions and muons) since they have low intensity and contain particles with limited lifetimes.

The main goal of this paper is to demonstrate an experimental method based on a conventional quadrupole scan [10] to measure the Twiss parameters of a muon beam offering so a viable approach to optimizing injection into the storage ring of the Muon g-2 Experiment. It is important to emphasize that to the best of the authors' knowledge this is the first time wherein such a measurement is applied to muon beams. It is also shown that the technique is capable of detecting variations in the design parameters. As an example, it is used to quantize the effect of scattering that is introduced from other diagnostic devices that are located upstream of the scan area. The outline of the paper is as follows. Sec. II gives an overview of the Muon Campus beamlines and its available instrumentation. The magnet scan technique is introduced in Sec. III and in Sec. IV the proof-of-principle experiment for the Muon campus is presented. Conclusions are presented in Sec. V.

II. OVERVIEW OF THE FERMILAB MUON CAMPUS

Figure 1(a) shows a schematic layout of the Fermilab Muon Campus. While a more detailed description of all Muon Campus beamlines can be found elsewhere [8], their main features are reviewed here. Protons with 8 GeV kinetic energy are transported via the M1 beamline to the target station at AP0 and produce a beam of secondary particles that is a mixture of different species but consists mainly of protons and pions. The target station consists of four main devices: a production target to generate secondaries, a lithium lens to focus secondaries, a pulsed magnet for energy selection, and a beam dump to remove unwanted particles. The target is made out of Inconel 600 (a nickel-iron alloy) cylinder with its center bored out for pressurized air to pass for internal cooling. A Beryllium outer shell keeps the target from spattering Inconel into the Lens.

The target assembly is positioned relative to the proton beam such that the beam subtends a chord of the cylinder. Transverse motion of the cylinder axis perpendicular to the beam allows the effective length of the target to be changed so that the target efficiency can be optimized. During full operation, 16 pulses of 10^{12} protons each within a 1.4 s cycle length are arriving at the target. The secondaries are focused by a lithium lens and then momentum-selected via a downstream pulsed dipole magnet (PMAG). The PMAG selects 3.1 GeV/c positive particles and bends them 3° into the M2-line channel. The M2-line is 50 m long and consist of series of 120° phase-advance FODO cells. Further downstream, a second dipole magnet provides another 3° bend to align the beam with the M3-line trajectory. The M3-line continues with a sequence of 90° phase-advance FODO cells for nearly 100 m, wherein a horizontal right bend, provided by a specialized insertion created from two 9.25° dipole bends, aligns the beam to the injection leg of the Delivery Ring (at $S = 160$ m). This line continues with another sequence of 72° phase-advance FODO cells for about 120 m, wherein the beam is injected vertically into the DR. The mixed secondary beam enters the DR (circumference 505 m) and circulates several turns to achieve a longitudinal separation between the protons and muons, due to the velocity difference between the different species. On the fourth turn, the longitudinal separation is sufficient for a fast kicker to cleanly remove the trailing proton beam.

Injection from the M3-line and extraction to the M4-line takes place in the same straight section (AP30) with the latter happening in the downstream half. Two kicker magnets are first used to kick the beam out of the closed orbit, then with the aid of a Lambertson magnet and a pair of two vertical bending magnets, the beam is extracted upward out of the DR. After traveling 30 m in the M4-line, the beam bends again upward into the M5-line and continues towards the storage ring of the Muon g-2 Experiment. The M5-line is 100 m long and includes a 27.1°

horizontal bend string halfway through which provides the proper entry position and angle into the muon storage ring. Right before the end of the M5-line there is a strong-focusing and highly tunable 10 m long final focus section, consisting of four quadrupole magnets, which provides optical matching to the storage ring.

Commissioning of the Fermilab Muon Campus begun in April 2017 and lasted for three months. The main goal of commissioning was to provide enough beam in the storage ring of the Muon g-2 Experiment to cross-check its detectors. Initially, an 8-GeV proton beam from the Recycler bypassed the target, then entered the DR via the M3 line and finally was extracted into the M4 line. The primary proton beam provided a good testbed for the optics and available beamline instrumentation, since its intensity is higher than the secondary beam by at least two orders of magnitude. More details of the incoming beam parameters can be found in Table I. Once confidence in the beam optics and instrumentation was established, the primary proton beam was sent to the target to commission the newborn 3.1-GeV secondary beam. To save experimental time, the secondary beam did not travel around the DR but rather passed straight through the AP30 section, then propagated down the M4/M5 lines, and into the storage ring of the Muon g-2 Experiment. This scenario is illustrated in Fig. 1(b) and will be focus of the remaining paper.

During commissioning, several devices [11] were available for monitoring the beam through the Muon Campus. The beam intensity was monitored with ion chambers (ICs), while the beam profiles were collected using secondary emission monitors (SEMs) and proportional wire chambers (PWCs). PWCs were more sensitive than SEMs, since they had the capability to measure beam intensities down to the 10^3 particle range. Each PWC assembly was filled with an 80% argon and 20% carbon dioxide gas mixture. Similar to SEMs and ICs, PWCs could be pulled out of the beam path when not in use in order to mitigate scattering effects from the gas mixture. The PWCs had two planes of signal wires, one plane for horizontal and one for vertical. There were 48 gold-plated tungsten signal wires in each plane with a 10 μm diameter and a 2 mm spacing. Table II shows all available devices along the direct path of the commissioning scenario starting from the target and extending all the way to the entrance of storage ring of the Muon g-2 Experiment.

Based on numerical simulations [9], the Muon Campus is expected to deliver 7.8x10^{-7} POT muons at the end of the M5 line during full operation. However, in the commissioning phase and since the DR is bypassed, the beam is contaminated with a mixture of muons, pions and protons. More specifically, the expected rates are: protons at 10^{-4} per POT, pions at 5.7x10^{-6} per POT and muons at 2.1x10^{-6} per POT.

III. MAGNET SCAN TECHNIQUE

The foundation of the magnet scanning technique discussed in this paper is the application of linear optics to beam transport and is a well-known method for measuring the transverse optics of particle beams [12, 13]. More specifically, a quadrupole magnet and a screen are used to obtain the emittance and Twiss parameters by measuring the beam size as a function of the quadrupole magnetic field strength at some imaging station a distance d further downstream. A schematic representation of the method is shown in Fig. 2.

It is common to describe a beam by its six-dimensional phase space, and we can consider the transverse properties of a beam in terms of two-dimensional phase spaces (x, x') and (y, y'), where x or y is the coordinate relative to the reference beam and x' and y' is the angular displacement of momentum in the x/z plane or y/z, respectively. Then, the area occupied by the particles can be considered as being bound by an ellipse expressed in terms of $\epsilon = \gamma x^2 +$

$2\alpha xx' + \beta x'^2$ wherein the Twiss parameters α, β, and γ describe the aspect ratio and orientation of the ellipse while the emittance ϵ describes the size of the ellipse [14]. If M is the transfer matrix of the scanning region, created by the product of the transfer matrices of drift S and quad Q, then the beam matrix at the screen σ_S is related to the beam matrix immediately upstream of the quadrupole σ_Q using the transformation $\sigma_S = M\sigma_Q M^T$, where the beam matrices in the horizontal direction are defined as $\sigma_Q = \epsilon\begin{pmatrix}\beta_{x,Q} & -\alpha_{x,Q}\\ -\alpha_{x,Q} & \gamma_{x,Q}\end{pmatrix}$ and $\sigma_S = \epsilon\begin{pmatrix}\beta_{x,S} & -\alpha_{x,S}\\ -\alpha_{x,S} & \gamma_{x,S}\end{pmatrix}$. After treating the quadrupole magnet as a thin lens with focal length f, we get $Q = \begin{pmatrix}1 & 0\\ -1/f & 1\end{pmatrix}$ and using $S = \begin{pmatrix}1 & d\\ 0 & 1\end{pmatrix}$ for the drift matrix we derive the following expression:

$$\beta_{S,x} = \beta_{Q,x}\left(1-\frac{d}{f}\right)^2 - 2\alpha_{x,Q}d\left(1-\frac{d}{f}\right)^2 + \gamma_{x,Q}d^2, \tag{1}$$

which can further be written in terms of the rms beam size $\sqrt{\langle x^2\rangle}$ at the screen:

$$\langle x^2\rangle_S = A\left(1-\frac{d}{f}\right)^2 - 2Bd\left(1-\frac{d}{f}\right) + Cd^2\ , \tag{2}$$

where $A = \beta_{x,Q}\epsilon_x$, $B = \alpha_{x,Q}\epsilon_x$, and $C = \gamma_{x,Q}\epsilon_x$ and $\epsilon_x = \sqrt{AC - B^2}$.

With this analysis in mind, the emittance and Twiss parameters can be obtained by a two-step process. First, the the beam size a given drift length after a quadrupole magnet is measured while scanning through a range of focusing strengths. Then, the rms beam size (squared) is plotted as a function of $(1 - d/f)$ and a parabolic fitting function is applied which will yield the three coefficients A, B, and C and thus will fully characterize the beam Twiss parameters and emittance. Similar analysis applies for the vertical plane as well. It is noteworthy to mention two points. First, the above equations assume zero dispersion and conserved emittance (Liouville's theorem). Second, it is desirable to be able to produce a beam waist over the range of quad strength values for the sake of accurate parabolic fitting.

IV. APPLICATION TO THE MUON CAMPUS

The quadrupole scan method is implemented at the final section of the M5 which is illustrated in Fig. 3. Note that the injection point to the storage ring is just 30 m downstream of PWC025. Magnets which are focusing and defocusing in the horizontal plane are colored as red and blue, respectively. Profiles are collected at PWC021 which is only ~10 m upstream of the entrance to the Muon g-2 Experiment storage ring. Thus, this provides a sweet spot not only to characterize the quality of the beam, but also to optimize it before injection into the storage ring. Since this technique relies on fitting a parabola, special care was taken to pass through a waist during the scans in both the horizontal and vertical planes. For this reason, we selected to scan Q020 and turned off magnet Q021. The distance between the front face of Q020 and PWC021 was 10 m which ensures enough drift for achieving a waist without any beam losses.

In order to benchmark our method, the aforementioned quadrupole scan process was simulated using the tracking code G4beamline [15] and the extracted Twiss parameters [using Eq. (2)] where compared against the ones calculated from the second order moments of the simulated beam distribution. The Twiss parameters calculated directly from the G4beamline distribution does not make the assumptions that the quadrupole scan process does (constant emittance, linear forces) and therefore can be used as a prototype to establish the quality of our measuring method. In both cases an agreement within 3% was found suggesting that our measurements are not impacted by nonlinear effects.

The experiment was then physically carried out, the focal length of Q020 was varied between 3 m and 7 m (design value is 3 m). Data collected at the PWC was fitted with a Gaussian (offset to account for noise) to obtain the rms beam width for each focal length and a parabola fitted to the appropriate plots. All fitting was performed in Python using SciPy's non-linear least squares fitting algorithm [17], which returns uncertainties on fitted parameters. A sample of the collected transverse profiles of the secondary beam is illustrated in Fig. 4. As we discussed in Sec II, our profile monitors have the capability to measure beam intensities down to the 10^3 range. Since we ran with 3.3x10^{11} protons on target our screens can capture the beam almost instantly. It is important to emphasize that the scanning process was fully automated and therefore the measuring process took only a few minutes.

Figure 5 shows the squared horizontal [Fig. 5(a)] and vertical [Fig. 5(b)] rms beam size as function of the Q020 magnet strength with a parabolic fit to the data (black dashed curve). Unlike the horizontal curve, the fit in the vertical plane is satisfactory at best. Next using Eq. (2) the Twiss parameters at the upstream face of Q020 can be determined. The results and corresponding uncertainties are illustrated in Table III for the horizontal and vertical planes. The measured horizontal and vertical emittances are 29 µm and 20 m, respectively. From inspection of Fig. 5 it is clear that the vertical fits are less accurate, and this is visible in the uncertainties in Table III; the average horizontal uncertainty is 6.4%, while the average vertical uncertainty is 15.8%.

During the experiment an activation area near PWC021 was discovered, indicating beam losses that were not predicted by the model. Further examination after shutdown revealed errors on the current settings in a group of quadrupole magnets along the first 25 m of the M5 section. Simulations later showed that such errors could introduce strong mismatches to the beam which can result in erratically behaving beta functions in the region of the quad-scan, which may be the source of the vertical uncertainty.

To the authors' knowledge, this is the first reported application of a quad-scan to a muon beam, as such it is important to verify the results obtained against other experimental measurements. One advantage of knowing the Twiss parameters is the ability to propagate them in both directions with linear optics. Since emittance is conserved the moments of the beam and rms width can be predicted, and in this case compared to results measured at other points in the beamline. Figure 6 shows that in the case of the g-2 experiment there is very good agreement between these predictions and the measured values in the horizontal plane [Fig. 6(a)], however there is some disagreement in the vertical plane [Fig. 6(b)]. This disagreement is likely related to the mismatching mentioned in the previous paragraph. Notice further that Figure 3 identifies Q019 as a defocusing magnet in the horizontal plane. As a result, the beam is expected to diverge and $\alpha_x < 0$ which is consistent with our measurement. For the same reason, the beam is expected to converge in the vertical plane and thus $\alpha_y > 0$ which is also consistent with our findings.

As discussed earlier in this paper, PWCs contain gas and can trigger beam losses from scattering. As an example of the power of the magnet scan technique, it can be used to quantize these scattering effects on the beam. In order to accomplish this, the aforementioned quadrupole scan experiment was repeated again, but this time with PWC301, PWC904, and PWC000 inserted into the path of the beam. Both cases are shown in Fig. 5. It is expected that the scattering from PWCs will generally increase the rms beam size and uncertainty as is seen, however this technique also provides information on how the Twiss parameters are affected, allowing for propagation further downstream. Table III shows the effect on the Twiss parameters. The technique allows quantification of the effect of PWCs; emittance grows from 29 μm to 32 μm in the horizontal plane and from 20 μm to 21 μm in the vertical plane when the PWCs are added to the beam, which is a notable increase that is difficult to quantify through other methods without additional equipment.

V. SUMMARY

In the upcoming years Fermilab is launching the Muon g-2 Experiment with the goal of determining with unprecedented precision the muon anomalous magnetic moment and thus study physics beyond the Standard Model. A combination of beamlines in the so-called Muon Campus have been designed to deliver beams sufficient for use in this experiment. Several studies have shown that the number of stored muons for the Muon g-2 Experiment is largely dependent on the injection parameters, specifically the Twiss parameters. Unfortunately, the current diagnostics in the Muon Campus beamlines allow only measurement of beam profiles which limits how well propagation can be predicted.

In this paper we have established a procedure to measure the Twiss parameters of a muon beam. The technique has been introduced and carried out on both a simulated and physical beamline. In both cases the results agree, and further comparisons with propagated beam widths support obtained values. The technique is extremely useful as it allows Twiss parameters to be measured with a reasonable uncertainty without the need to add any new equipment to the beamline. The proximity of the measured region to the entrance of the storage ring makes this technique a promising approach to optimizing injection for the Muon g-2 Experiment. During commissioning this initial quad-scan has already proved useful; it diagnosed a discrepancy between design and obtained results and further investigation into the beamline revealed errors in some of the magnet settings upstream of the scan which has been now corrected.

ACKNOWLEDGEMENTS

We are grateful to Andrew Fiedler for his help carrying out the experiment, and Mike Syphers for much useful guidance and discussion. This work is supported by Fermi Research Alliance, LLC under Contract No. De-AC02-07CH11359 with the United States Department of Energy

REFERENCES

[1] muon.fnal.gov.

[2] J. Grange *et al.*, “Muon (g-2) Technical Design Report,” arXiv:1501.06858, (2015).

[3] G. W. Bennett *et al.,* Phys.Rev. D **73**, 072003 (2006).

[4] W. Gohn, “The muon g-2 experiment at Fermilab,” arXiv:1611.04964, (2016).

[4] C. Yoshikawa et al., Optimization of the target subsystem for the new g-2 Experiment, in Proceedings of the 3rd

[5] D. Stratakis et al., Proceedings of IPAC 2017, Copenhagen, Denmark, p. 4505 (2017)

[6] Design report Tevatron 1 project, Report No. FERMILABDESIGN- 1984-01.

[7] D.W. Hertzog, Next Generation Muon g-2 Experiments, Eur. Phys. J. Web Conf. 118, 01015 (2016).

[8] D. Stratakis *et al.,* Proceedings of IPAC 2016, Busan, p. 996 (2016).

[9] D. Stratakis et al. Phys. Rev. Accel. Beams **20**, 111003 (2017).

[10] M. Minty and F. Zimmerman, Measurement and Control of Charged Particle Beams, Springer-Verlag, Berlin (2013).

[11] B. Drendel, G Minus 2 Experiment Document 4590 (2016), https://gm2-docdb.fnal.gov/

[12] B. E. Carlsten et al., Nucl. Instrum. Methods Phys. Res., Sect. A 331, 791 (1993)

[13] S. Bernal, “Beam emittance and emittance measurement”, US Particle Accelerator School (USPAS), 2008, University of Maryland.

[14] D. A. Edwards and M. J. Syphers, An Introduction to the Physics of High Energy Accelerators (John Wiley & Sons, New York, 1993).

[15] http://www.muonsinternal.com/muons3/G4beamline

[16] D. Stratakis, “Quad-Scan", G Minus 2 Experiment Document, GM2-doc-6764-v1 (2017), https://gm2-docdb.fnal.gov/

[17] SciPyDocs, https://docs.scipy.org/doc/scipy/reference/generated/scipy.optimize.curve_fit.html

[18] S. Kim, D. Rubin, D. Stratakis, and N. S. Froemming, Proceedings of NAPAC 2016, p. 803 (2016).

.

TABLE AND FIGURE CAPTIONS

Table I: Primary beam parameters

Parameter	**Value**
Intensity per pulse	$3.3\text{x}10^{11}$
Bunch length (ns)	120
Bunch separation (s)	10
Primary Momentum (GeV/c)	8.89
Beam size at target (mm x mm)	0.25x0.33

Table II: Location of available beam diagnostics for the commissioning scenario in Fig. 1 (b).

Beamline	S (m)	Type	Detector ID
M2	20.45	IC	804
M2	21.02	SEM	804
M2	37.98	SEM	810
M3	51.76	SEM	706
M3	77.26	SEM	711
M3	121.30	SEM	719
M3	163.41	SEM	726
M3	173.24	SEM	729
M3	234.83	SEM	740
M3	235.21	IC	740
M3	258.98	PWC	744
M3	269.00	PWC	748
DR	296.08	PWC	301
DR	306.34	PWC	204
M4	312.31	PWC	900
M4	320.74	IC	902
M4	325.11	PWC	904
M5	341.75	PWC	000
M5	355.57	PWC	005
M5	368.78	PWC	011
M5	383.96	PWC	014
M5	417.53	PWC	020
M5	424.33	PWC	021
M5	436.30	PWC	025
M5	436.50	IC	025

Table III: Measured Twiss parameters at the upstream face of Q020. To investigate the scattering effect the measurement was made with monitors PWC301, PWC904, and PWC000 inserted along the beam path (PWCs column) and without (No PWCs column).

Twiss Parameter	x		y	
	PWCs	No PWCs	PWCs	No PWCs
Alpha, α_Q	-4.8 ± 0.4	-4.6 ± 0.3	2.2 ± 0.4	2.4 ± 0.4
Beta, β_Q /m	26.7 ± 2.2	25.9 ± 1.8	9.9 ± 1.4	10.7 ± 1.6
Gamma, γ_Q /m^{-1}	0.88 ± 0.06	0.86 ± 0.05	0.61 ± 0.09	0.64 ± 0.10

FIGURE CAPTIONS

FIG. 1 (Color online): A schematic representation of the Muon Campus accelerator complex that is used by the Muon g-2 Experiment. Secondaries are produced on a target then travel through the M2-and M3-line, which is designed to capture as many 3.1 GeV/c muons from pion decays as possible. The beam is injected into the DR wherein a kicker is used to remove the protons, the resulting muon beam is then extracted into the M4-line, and the muon beam is eventually transferred to the new M5-line that leads to the muon storage ring. The combined M2-and M3-line and M4-and M5-line lengths are 280 m and 130 m respectively, and the DR that has a circumference of 505 m. (a) The full operation scenario wherein the beam is doing four turns in the DR before extraction into the M4, and (b) The commissioning scenario described in this study, wherein the beam is not doing any DR turns but is rather passing through a straight section of the DR. Note that the storage ring of the Muon g-2 Experiment is enclosed in the MC-1 building.

FIG. 2 (Color online): Simplified diagram showing the principle of the magnet scan technique.

FIG. 3 (Color online): Final stretch of the M5 beamline of the Fermilab Muon Campus. Injection to the storage ring (not shown here) of the Muon g-2 Experiment starts 30 cm downstream of PWC025. Blue and red distinguish the quadrupoles that are focusing and defocusing in the horizontal plane.

FIG. 4 (Color online): Horizontal (red) and vertical (blue) beam profiles collected at PWC021 for different focusing strengths f, of magnet Q020. To avoid beam losses, magnet Q021 is turned off.

FIG. 5 (Color online): Squares of rms beam size vs focusing strength and fit using Eq. (2). (a) Beam horizontal projection. (b) Beam vertical projection. The fit (dashed line) provides information on the transverse beam optics and thus allows the tuning and optimization of injection in the storage ring of the Muon g-2 Experiment. The measurement was made with monitors PWC301, PWC904, and PWC000 inserted along the beam path (red) and without (black). The scattering induced from the aforementioned monitors makes the beam size larger.

FIG. 6 (Color online): (a) Comparison of the measured by the profile monitors and (quad-scan) propagated horizontal beam widths. Furthest value extrapolated from half profile due to noisy wires, and (b) Comparison of measured and (quad-scan) propagated vertical beam widths.

Figure 1

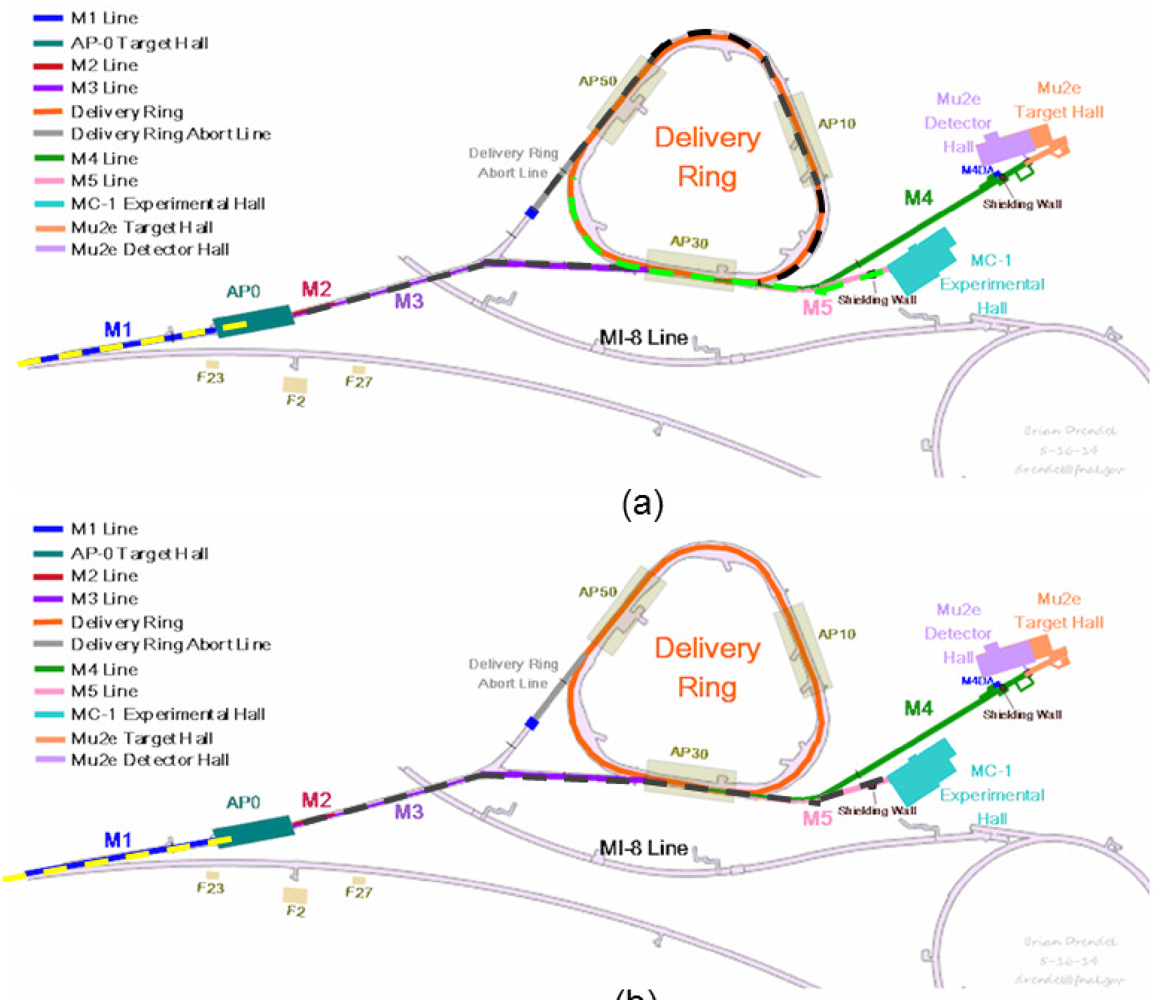
M1 Line
AP-0 Target Hall
M2 Line
M3 Line
Delivery Ring
Delivery Ring Abort Line
M4 Line
M5 Line
MC-1 Experimental Hall
Mu2e Target Hall
Mu2e Detector Hall
AP50
AP10
AP30
Delivery Ring
Delivery Ring Abort Line
Mu2e Detector Hall
Mu2e Target Hall
M4DA
Shielding Wall
M4
MC-1 Experimental Hall
Shielding Wall
M5
AP0
M1
M2
M3
MI-8 Line
F23
F2
F27
Brian Drendel 5-16-14 drendel@fnal.gov

(a)

(b)

Figure 2

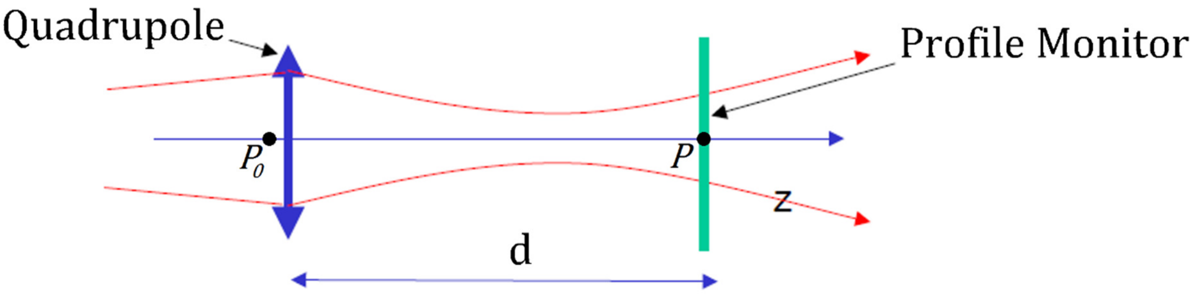

Figure 3

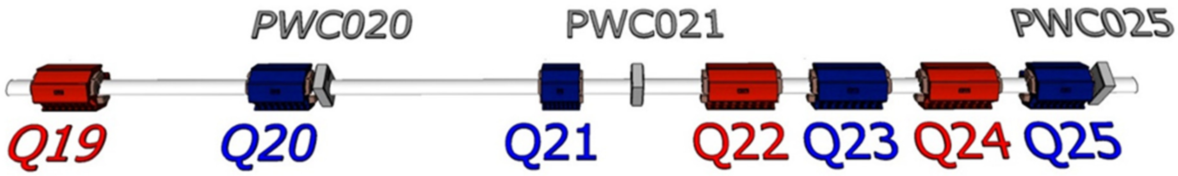

Figure 4

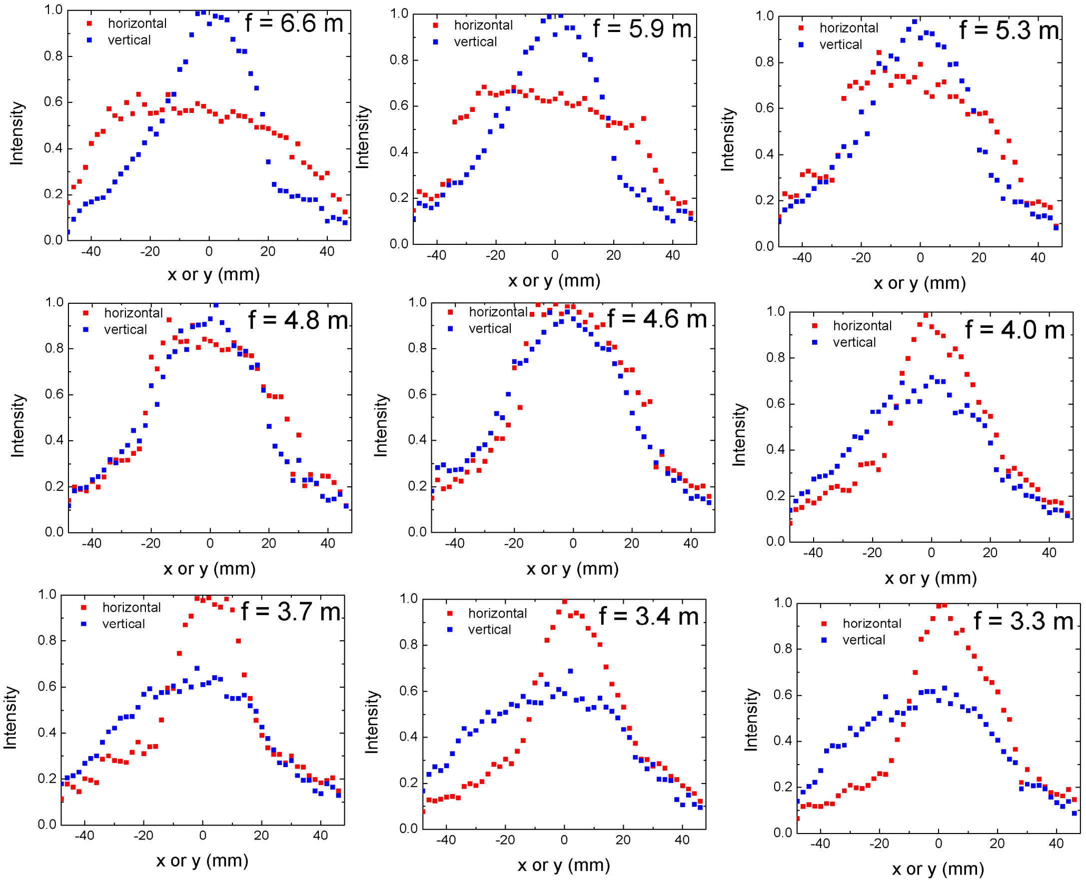

horizontal
vertical
f = 6.6 m
f = 5.9 m
f = 5.3 m
f = 4.8 m
f = 4.6 m
f = 4.0 m
f = 3.7 m
f = 3.4 m
f = 3.3 m
Intensity
x or y (mm)
0.0
0.2
0.4
0.6
0.8
1.0
-40
-20
0
20
40

Figure 5

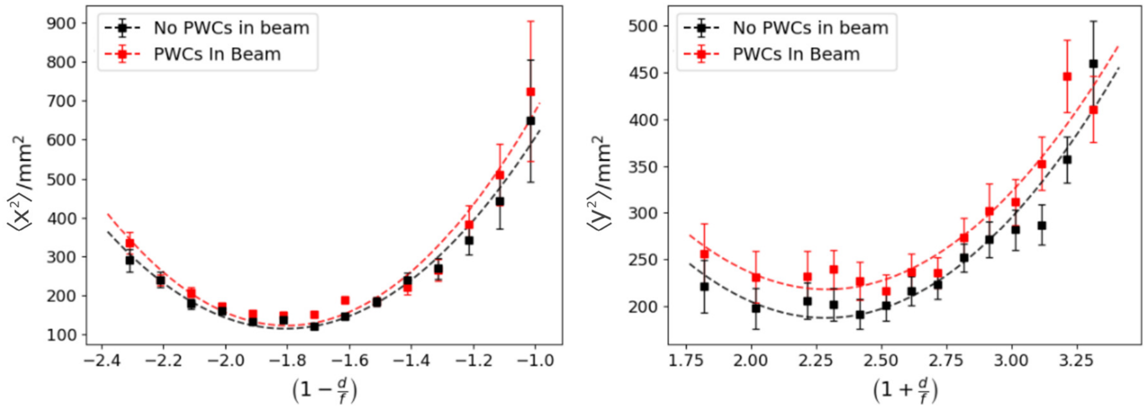
No PWCs in beam
PWCs In Beam
⟨x²⟩/mm²
900
800
700
600
500
400
300
200
100
−2.4
−2.2
−2.0
−1.8
−1.6
−1.4
−1.2
−1.0
(1 − d/f)
No PWCs in beam
PWCs In Beam
⟨y²⟩/mm²
500
450
400
350
300
250
200
1.75
2.00
2.25
2.50
2.75
3.00
3.25
(1 + d/f)

(a) (b)

Figure 6

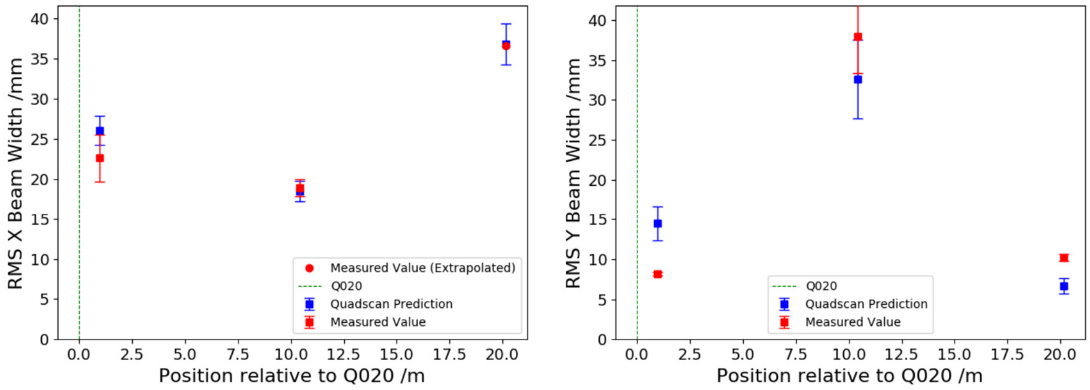
RMS X Beam Width /mm
0
5
10
15
20
25
30
35
40
0.0
2.5
5.0
7.5
10.0
12.5
15.0
17.5
20.0
Position relative to Q020 /m
Measured Value (Extrapolated)
Q020
Quadscan Prediction
Measured Value
RMS Y Beam Width /mm
0
5
10
15
20
25
30
35
40
0.0
2.5
5.0
7.5
10.0
12.5
15.0
17.5
20.0
Position relative to Q020 /m
Q020
Quadscan Prediction
Measured Value

(a) (b)